Published in final edited form as:
Acta Biomater. 2013 April ; 9(4): 6095–6104. doi:10.1016/j.actbio.2012.12.028.

Primary Human Chondrocyte Extracellular Matrix Formation and Phenotype Maintenance using RGD-derivatized PEGDM Hydrogels Possessing a Continuous Gradient in Modulus

Laura A. Smith Callahan[1], **Anna M. Ganios**[1], **Erin P. Childers**[1], **Scott D. Weiner**[2], and **Matthew L. Becker**[1,3,4,*]

[1]Department of Polymer Science, The University of Akron, Akron, OH

[2]Department of Orthopedic Surgery, Summa Health Systems, Akron, OH

[3]Center for Biomaterials in Medicine, Austen Bioinnovation Institute in Akron, Akron, OH

[4]Akron Functional Materials Center, Akron, OH

Abstract

Efficient *ex vivo* methods for expanding primary human chondrocytes while maintaining phenotype is critical to advancing autologous cell sourcing efforts for tissue engineering applications. While there is significant activity in the literature, systematic approaches are necessary to determine and optimize the chemical and mechanical scaffold properties for hyaline cartilage generation using limited cell numbers. Functionalized hydrogels possessing continuous variations in physico-chemical properties are therefore an efficient three-dimensional platform for studying several properties simultaneously. Herein, we describe a polyethylene glycol dimethacrylate (PEGDM) hydrogel system possessing a gradient in modulus (~27,000 Pa to 3,800 Pa) containing a uniform concentration of arginine–glycine–aspartic acid peptide (RGD) to enhance cellular adhesion for the correlation of primary human osteoarthritic chondrocyte proliferation, phenotype maintenance, and ECM production to the hydrogel properties. Cell number and chondrogenic phenotype (CD14:CD90 ratios) were found to decline in regions with higher storage modulus (>13,100 Pa), while regions with lower storage modulus maintained cell number and phenotype. Over three weeks of culture, hydrogel regions possessing lower storage modulus experience an increase in ECM content (~200%) compared to regions with higher storage modulus. Variations in the amount and organization of cytoskeletal markers actin and vinculin were observed within the modulus gradient which are indicative of the differences in chondrogenic phenotype maintenance and ECM expression. Thus scaffold mechanical properties significantly impact on modulating human osteoarthritic chondrocyte behavior and tissue formation.

Keywords

Cartilage; Tissue Engineering; Hydrogel; combinatorial methods; gradient

* Corresponding Author Department of Polymer Science The University of Akron Akron, OH 44325-3909 Phone: 330-972-2834 Fax: 330-972-5290 becker@uakron.edu.

1. Introduction

The Osteoarthritis Research Society International Disease State working group with the United States Food and Drug Administration has determined that future OA treatments should focus on preserving the joint and addressing the underlying mechanical changes in cartilage during OA progression.[1] While stem cell technology holds great promise for the future, utilizing autologous cell sources sidesteps many of the issues related to ethics in sourcing, safety and compatibility faced by researchers in the near term. Significant limitations in using OA chondrocytes for regenerative medicine applications are their low numbers and metabolic imbalance between expression of catabolic matrix cytokines and synthesis of extracellular matrix (ECM), which is exacerbated by increasing degradation of the ECM.[2-4] For autologously-sourced OA chondrocytes to be a viable option for tissue engineering applications, optimal *ex vivo* conditions must be developed to expand the number and bioactivity of these cells while preserving the narrow cellular phenotype necessary for implantation.

Tissue engineering offers the potential to meet these requirements and lead to the generation biomimetic hyaline cartilage with mechanical properties identical to native materials. However, this ideal scaffold has yet to be developed. To expedite scaffold development, combinatorial methods, long used in the pharmaceutical industry, have been adapted for biomaterials and tissue engineering.[5, 6] Many combinatorial methods have been developed for two dimension culture (2D) instead of three-dimensional (3D) culture which is more similar to the native tissue environment.[7] One strategy, which can be adapted easily to 3D culture, while maximizing the number of material conditions tested, is a continuous hydrogel gradient.[8-10] The combinatorial approach minimizes variability in cell sourcing, seeding density and chemical heterogeneity. As such, a continuous hydrogel gradients system will be used to systematically screen the effect of hydrogel mechanical properties on OA chondrocyte behavior.

Cartilage is a mechanically complex and heterogeneous tissue which exhibits changes in mechanical properties during development,[11] in a zonal manner through its depth,[12, 13] and spatially around chondrocytes.[14-16] The local stiffness of the pericellular matrix, the ECM closest to chondrocytes, is at least an order of magnitude lower than that of the bulk cartilage ECM in adult tissue.[14-16] The locally lower stiffness near the chondrocytes coupled with recent studies indicating that culturing stem cells on materials with reduced stiffness enhance chondrogenic differentiation compared to that of stem cells cultured on stiffer materials[17, 18] indicates that scaffolds of lower modulus than those reported previously should be examined for cartilage tissue engineering.[19-21] However it remains highly unlikely that a single modulus material will provide a solution to the challenges we have outlined. Previous studies on the effect of matrix mechanical properties on chondrogenesis have not utilized gradient approaches allowing them to only examine a few discrete samples providing limited data.[20-23]

We hypothesize through emulating the mechanical properties of softer immature cartilage bulk ECM approaching the stiffness of the pericellular matrix with poly (ethylene glycol) dimethacrylate (PEGDM) gels will enhance cartilage formation from OA chondrocytes. PEGDM hydrogel matrices are relatively bio-inert, providing structural support to cells without direct biological signaling. To enhance the chondrocytes ability to detect changes in mechanical properties over the gradient, an arginine– glycine–aspartic acid peptide (RGD), an integrin binding sequence found in several ECM proteins,[24, 25] will be incorporated into the PEGDM hydrogels at a constant concentration. In these studies, primary human chondrocytes from middle age patients undergoing total knee replacement were cultured in RGD-functionalized PEGDM hydrogels possessing a gradient in storage modulus created

through mass fraction variations. Chondrocyte proliferation, phenotype maintenance, and ECM production were systematically screened over 3 weeks of *in vitro* culture

2. Experimental Methods

2.1 Cell Isolation

All studies involving human tissue were IRB-approved at each of the institutions involved. Chondrocytes were isolated from the tibial plateaus and femoral condyles of patients undergoing total knee arthoplasty (average age: 52.2 yrs, range: 46-55 yrs, total knees (female): 9(6)). Isolated tissue was placed in 4 mg/mL collagenase in Hank's buffered salt solution for at least 4 h and washed twice with phosphate buffered saline (Invitrogen, Carlsbad, CA). Human chondrocytes were then passed through a 22 mm diameter stainless steel syringe **filter (~80μm)** to remove cellular debris and encapsulated in hydrogels immediately after isolation.

2.2 RGD Synthesis

GRGDS (RGD) was synthesized using standard solid-phase FMOC chemistry on Wang's resin. A photopolymerizable acrylate group was coupled to the N-terminus of each peptide during synthesis. Peptides were cleaved from the resin using standard conditions (45 m, 95% trifluoroacetic acid, 2.5% triisopropylsilane, 2.5% water (all vol.%)) and precipitated in diethyl ether. Following two trituration cycles, the peptides were dialyzed in deionized water (molecular mass (MW) cutoff 100-500 Da, cellulose ester, Spectrum, Rancho Domingo, CA), and the formal weight was verified with matrix-assisted laser desorption ionization–time of flight (MALDI-TOF). (FW (acrylic acid-GRGDS) = 545.3 g mol^{-1}).

2.3 Hydrogel Fabrication

Solutions (5%, 15% and 50%) of PEGDM (~8000 g/mol) (Monomer-Polymer & Dajac Labs, Trevose, PA) in Opti-MEM were prepared containing 0.1% Irgacure 2959 (Ciba Specialty Chemicals, Basel, Switzerland). Solutions were loaded into 1 mL syringes and placed in a computer driven syringe pump system (Figure 1A & 1B) to create gradient hydrogels (Figure 1C). Computer controlled syringe pumps were used to dispense 15% and 50% PEGDM solutions in inverse ramping profiles ranging from 53 mL/hr to 0 mL/hr over 90 s into a custom mold while 5% PEGDM solution was dispensed at a constant rate of 10 mL/hr (Figure 1D). The mold possessed a depth profile (1 mm) to minimize diffusional mixing during gradient formation. Hydrogels were photopolymerized using ~2.3 mJ/cm^2 UVA light for 5 min and then placed in Opti-MEM I reduced-serum medium for storage. Unless otherwise noted, all samples for analysis were 5 mm by 10 mm by 1 mm. For cellular experiments, 5% PEGDM solution contained 2.52 mM RGD and 3.85×10^6 cells/mL leading to a final RGD concentration of 400μM and cell content of 777,700 cells per gradient. The profiles were designed to ensure uniform cell density within the gradient specimen. Cellular samples were cultured up to 3 weeks in Opti-MEM I reduced-serum medium containing 50 μg/mL ascorbate and 100 μg/mL primocin at 37 °C in a 5% CO_2 incubator. Then media was exchanged every other day.

2.4 Hydrogel Characterization

For swelling studies, samples were weighed and measured dimensionally immediately after photopolymerization. The hydrogels were then placed in Opti-MEM at 37 °C in a 5% CO_2 incubator for 24 h. Following incubation, the samples were blotted dry before being weighed and measured again. The samples were then placed on a freeze dryer and thoroughly dried before being weighed again. Swelling ratio, q, was determined by taking the ratio of the swollen mass of the hydrogel by the mass of the hydrogel after lyophillization. The mesh

size was determined as described by Canal and Peppas[26] using the equation $\xi = V_{2,s}^{-\frac{1}{3}} l C_n^{\frac{1}{2}} n^{\frac{1}{2}}$ with the alteration proposed by Anseth[27] and Hubbel.[28] $V_{2,s}$ is the equilibrium polymer volume fraction in the gel, l is the bond length (1.50Å),[28] C_n is the characteristic ratio of PEG,[29] and n is the number of bonds between crosslinks.

To determine the storage modulus, 8 mm diameter samples were punched from gradients every 10 mm with a gasket punch and tested on a ARES-G2 rheometer (TA Instruments, Newcastle, DE) using 8 mm serrated parallel plates with a strain amplitude of 1% and 30N constant normal force to prevent slippage over an angular frequency sweep from 100 to 1 rad/s with 10 points per decade. Modulus data are reported at an angular frequency of 1 rad/s as the gels did not show frequency dependent response.

To determine the Young's and shear modulus, 5 mm gradient sections were tested on a TA.XTplus texture analyzer (Stable Micro Systems, Surrey, England) with a ¼ in spherical probe. The probe penetrated the gels at a constant velocity of 0.01 mm/s. Force (N), depth (mm), time (s) and strain data were collected. The contact radius (equation 1),[30] indentation stress (equation 2),[30] Young's modulus(equation 3)[30] and shear modulus (equations 4)[31] were calculated using the following equations.

$$a = R^{1/2}\delta^{3/2} \text{ where } R \text{ is the radius of indentor and } \delta \text{ is depth of indentions} \quad \text{(Equation 1)}$$

$$\sigma = F / \left(\pi a^2\right) \text{ where } F \text{ is applied force.} \quad \text{(Equation 2)}$$

$$E = \sigma 3\pi (1 - v) / (20\varepsilon) \text{ where } v \text{ is poisson ration of polyethylene glycol and } \varepsilon \text{ is strain} \quad \text{(Equation 3)}$$

$$G = 3P_i / (16afp((\sqrt{R\delta})/h)) \text{ where } P_i \text{ is the load response and } fp((\sqrt{R\delta})/h)) = ((\sqrt{R\delta})/h)^2 + 0.82((\sqrt{R\delta})/h) + 0.46 / (((\sqrt{R\delta})/h) + 0.46) \text{ where } h \text{ is height of the hydrogel} \quad \text{(Equation 4)}$$

The bioavailability of RGD was determined in a manner similar to one previously described using a peptide designed to mimic the natural integrin receptor (CWDDGWLC-biotin) (American Peptide, Sunnyvale, CA) and Alexaflour 488 streptavidin colloidal gold (Invitrogen).[32] Briefly, samples were blocked for 1 h with bovine serum albumin in RGD blocking buffer, washed for 5 min in RGD wash buffer 5 times, and incubated overnight at ambient temperature on an orbital shaker at ~75 rpm in 0.1 mg/mL integrin mimicking peptide in RGD wash buffer. Samples were washed 5 more times for 5 min each in RGD wash buffer to remove unbound peptide and incubated in 3 ng/mL Alexaflour 488 streptavidin colloidal gold overnight at ambient temperature on an orbital shaker at ~75 rpm. Samples were washed 5 times for 5 min each in RGD wash buffer to remove unbound Alexaflour 488 streptavidin colloidal gold and then viewed on a IX81 microscope (Olympus, Center Valley, PA).

2.5 Histological Staining and Immunohistochemistry

All samples were fixed overnight in 4% paraformaldhyde (Sigma). Whole mount histological staining samples were transferred to PBS and stained with 0.5% Alcian blue (Sigma) for 3 h at room temperature. Samples were then washed with PBS and water and imaged on a CKX41 microscope (Olympus). Whole mount samples for CD14 (SC9150,Santa Cruz, 1:100) and CD90 (SC6071, Santa Cruz, 1:100) were washed in PBS thrice for 5 min each and once in .1% donkey serum with 0.01% sodium azide in PBS for 30

min at room temperature. Donkey serum (10%) was used to block for 1 h. Samples were incubated in primary antibodies overnight then stained with appropriate alexaflour secondary antibodies and DAPI for 1 h, washed and then viewed. J Image (downloaded from the National Institute of Health, Bethesda, MD, USA, free download available at http://rsb.info.nih.gov/ij/) was used to determine the frequency of CD14 and CD90 in the cell population for at least 90 cells from 3 separate gradients at each position. The fraction of cells in the total cell population expressing CD14 and CD90 was determined. The CD14/CD90 ratio was obtained by then dividing the fraction of cells in the total poplulation expressing CD14 by the faction of cells in the total cell population expressing CD90. These values were then normalized to the day 10 45mm gradient position.

Whole mount cytoskeletal staining samples were transferred to 0.5% Triton x-100 in cytoskeleton stabilization (CS) buffer (0.1 M PIPES, 1 mM EGTA, and 4% (w/v) 8000 MW polyethylene glycol) at 37 °C for 10 min, rinsed thrice for 5 min each in CS buffer, and incubated in 0.05% sodium borohydride in PBS at ambient temperature for 10 min. Whole mount samples were then blocked in 5% donkey serum for 20 min at 37 °C and incubated overnight at 4 °C with vinculin antibody (V4505, Sigma, 1:100) and rhodamine phalloidin (1:200). Samples were then washed thrice with 1% donkey serum for 5 min, followed by appropriate secondary antibodies conjugated to FITC. DAPI was used to stain the cell nuclei. Samples for histological sectioning were transferred to 70% ETOH for at least 1 h, 80% ETOH for 1.5 h, 95% ETOH for 12 h, ETOH for 1.5 h twice and xylene for 1 h. Samples were then placed in a 60 °C paraffin bath for 12 h and embedded in a paraffin block for sectioning.[33] Blocks were removed from a −20 °C freezer and cut into 7 μm sections. After 2 days of drying in a 37 °C oven, samples were stained with picro-sirius red solution with Mayer's haematoxylin (Fisher Biological, Pittsburgh, PA) after paraffin removal with xylene and rehydration through an ethanol gradient. After rehydration, immunochemistry samples were incubated in 0.5% pepsin for 10 min at 30 °C for antigen retrieval. Nonspecific antibody binding was blocked by incubating in 10% goat serum, then samples were exposed to collagen type 2 (Col 2) (1:200) and collagen type 1A (Col 1A) (1:100) antibodies or matrix metalloprotease 13 (MMP-13) (1:50) and matrix metalloprotease 3 (MMP-3) (1:30), followed by appropriate secondary antibodies conjugated to alexaflour 488 (Col 2, MMP-13) or alexaflour 546 (Col 1A, MMP 3). . DAPI was used to stain the cell nuclei. The Col 2 antibody (II-II6B3) developed by Thomas F. Linsenmayer was obtained from the Developmental Studies Hybridoma Bank developed under the auspices of the NICHD and maintained by The University of Iowa, Department of Biology, Iowa City, IA 52242. The Col 1A (sc-25974), MMP 13 (sc-12363), and MMP 3 (sc-21732) antibodies were obtained from Santa Cruz Biotechnology (Santa Cruz, CA) and DAPI was obtained from Sigma. J Image was used to determine the mean gray scale intensity for col 2, col 1A, MMP 13, and MMP 3 surrounding the cell population for at least 20 cells from 3 separate gradients at each position. The average number of cells per μm^2 in histological sections was determined from nuclear staining in at least 30 images from 3 separate gradients at each position..

2.6 Biochemistry

Samples were homogenized with a Tissue-Tearor (BioSpec Products, Inc., Bartlesville, Oklahoma). DNA content was determined with a fluorescence assay from Sigma according to manufacture protocol. Sulfated gylcosaminoglycans (sGAGs) were quantified with dimethylmethlene blue (DMB) or Alcian blue extraction, while collagen content was quantified using dimethylaminobenzaldehyde (DAB) to observe chloramines T-oxidized hydroxyproline as previously described.[34-37] Briefly, homogenized sampleswere digested with proteinase K overnight at 60 °C. Samples for sGAGs detection were added to DMB solution at ratio of 1:10, mixed and read at 535 nm. The absorbance was converted to μg of

GAG based on absorbance reading from a standard curve of chondroitin sulfate. Samples for hydroxyproline detection were dehydrated, autoclaved at 120 °C with 2N NaOH for 20 min, oxidized with chloramine T solution for 25 min at room temperature on an orbital shaker at 100 rpm and then incubated with DAB for 20 min at 65 °C. The absorbance was then read at 550 nm and converted to μg of hydroxyproline based on a standard curve of hydroxyproline. For Alcian Blue quantification of sGAGs from whole mount histological staining samples, samples were destained in 3% acetic acid twice, washed twice in PBS and the dye extracted with 8M guanidine HCl overnight at ambient temperature[38, 39]. The supernatant was centrifuged and the absorbance read at 600 nm. GAG concentrations were determined from a standard curve of chondroitin sulfate, which was stained according to the Alcian Blue protocol described above, and centrifuged for 10 minutes at 16000g at 4°C to form a pellet. The supernant was removed and the pellet was gently washed with PBS and the dye extracted according to the protocol described above[36].

2.7 Statistics

All experiments were conducted at least 3 times ($n \geq 3$). All quantitative data are presented as the average ± standard deviation. One-way analysis of variance (ANOVA) with Tukey post hoc analyses and correlation analysis with linear regression were performed where applicable. Significance was set at a p-value of less than 0.05.

3. Results

The Young's Modulus increases from 2050 Pa ± 420 Pa (average ± std) to 6110 Pa ± 1140 Pa (average ± std), the shear modulus increases from 87,700 Pa ± 17,600 Pa to 243,900 Pa ± 45,700 Pa and the storage modulus increases from 3,770 Pa ± 800 Pa Pa to 27,200 Pa ± 1170 Pa (Figure 2) down the length of the gradient. Based on the correlation of storage modulus to known PEGDM concentration (Figure 1) the gradient hydrogel samples range in composition from 9.5% ± 6.4% (average ± std) in the 0 mm position to 30.4% ± 6.4% at the 40 mm position indicating that the gradient spans the commonly reported PEGDM concentrations for cartilage tissue engineering.[18, 20, 23, 40, 41] This decrease in PEGDM content leads to increased swelling and mesh size down the gradient (Figure 2C). However, after 10 days of culture containing encapsulated chondrocytes the swelling ratio was reduced to 7.0 ± 0.5 with a water content of 84.5% ± 1.0% across all gradient positions. The pre-encapsulation water content of the gradient ranged from 92.5% ± 0.9% to 87.3% ± 0.3%. The reduction in swelling ratio and water content after 10 days of chondrocyte culture across the entire gradient has brought every position regardless of PEGDM content much closer to that of normal human cartilage, which are 5% and 80% respectively.[42] The bioavailability of RGD peptide within the gradient was detected using an integrin mimicking peptide. A constant level of bioavailable RGD was measured throughout gradient (Data not shown).

Over the course of 10 days of *in vitro* culture, chondrocytes encapsulated at the 6500 Pa Young's Modulus gradient position, which has the highest modulus, experienced a significant decrease in total DNA content indicating cell death compared to areas with lower modulus which experienced a significant increase or no change in DNA content (Figure 3A). Over the same time course, the ratio the surface marker CD14 (a lipopolysaccharide receptor found on freshly isolated chondrocytes[43, 44]), expression to that of surface marker CD90 expression (glycosylphosphatidylinositol-anchored glycoprotein associate cellular proliferation[43, 45], which is present at low amounts on freshly isolated chondrocytes[44]) was used to quantify chondrocyte phenotype maintenance.[43, 46, 47] The CD14/CD90 ratio decreased over the time course at all gradient positions (Figure 3B). This reduction in phenotype is mainly due to the reduced expression of CD14 across the gradient (Figure 3C), since CD90 is expressed at a fairly constant level over the examined time course (Figure 3D). As cytoskeletal organization has been shown to play a role in

chondrocyte behavior,[48-50] the organization of actin and vinculin were examined. After 5 days of encapsulation, the actin and vinculin organization varied depending on Young's modulus (Figure 4). Changes in cytoskeletal organization have previously been linked to alterations in ECM synthesis.[48, 49, 51] After 10 days of encapsulation, lower Young's modulus regions with chondrocytes contained more sGAGs than higher storage modulus containing regions (Figure 5). After 3 weeks of culture, this trend continues with lower Young's modulus regions containing more sGAGs than higher storage modulus regions (Figure 6A, 6D & 7A). Higher collagen content was found in regions with lower Young's modulus compared to regions with higher storage modulus (Figure 6B, 6C, 6D, 7B, & 7D). Increased Col 2, the principle collagen in the cartilage ECM, was found in regions with lower Young's modulus compared to regions with higher Young's modulus (Figure 6C & 7D). However, Col 1A, a marker of dedifferentiation, increased in a similar manner (Figure 6D & 7D). MMP 13 and MMP 3, which primarily degrade col 2 and proteoglycans respectively, exhibited decreased staining in regions with lower Young's modulus compared to regions with higher Young's modulus (Figure 6E, 6F, & 7D). Cellular number was also examined at the 3 week time point and was found to be similar for most gradient positions (Figure 7B). The 1700 Pa Young's modulus gradient position, with the lowest storage modulus, was found to contain significantly more cells than the 30 mm and 40 mm gradient positions.

4. Discussion

Rationally optimizing scaffold design remains a major challenge in tissue engineering.[52] A number of physical properties such as topography,[34, 53] porosity[54] and stiffness[55] have been found to modulate cell behavior and tissue formation. Three dimensional hydrogel gradients represent a straightforward way to systematically study many of these properties to determine optimal conditions for tissue formation. In these studies we have developed and characterized a gradient hydrogel system for the study of mechanical property changes on OA chondrocyte behavior.

The Young's modulus of chondrocytes has been reported as 660 Pa, while the Young's modulus of pericellular matrix around healthy chondrocytes has been reported as 1540 Pa.[15] Both reports are significantly lower than the Young's modulus reported of ~0.699 MPa for fetal human articular cartilage[56] and are near the stiffness regime of our gradients (Figure 2A). Gels possessing lower mechanical properties were not pursued due to the inability to transfer the gradients intact for cell culture. Additionally, mature cartilage is estimated to have a pore size of 60Å,[57] which encompasses the range of mesh sizes generated within our gradient (Figure 2C) indicating that the gradient should possess mass transport capabilities sufficient to maintain chondrocyte viability.

The number of chondrocytes within all gradient regions is similar after 1 day of culture indicating that cells were originally encapsulated at a similar density throughout the gradient. The low observed proliferation rate in this study was most likely due to the short culture time. A previous study in PEG hydrogels used a culture period 3 times longer in order to show increased proliferation of human OA chondrocytes.[41]

As the modulus was modified by increasing polymer mass fraction, reduced mass transport could contribute to differences in cellular response observed across the gradient (Figure 3A). However, since the decrease in cellular content occurred at the end of the gradient where additional surface area is available to facilitate mass transport compared to the adjacent segment which experienced proliferation, it is unlikely that differences in molecular diffusion within the segments played a significant role in these results. Previous studies utilizing similar PEG hydrogel systems report conflicting results on the solute diffusion

capabilities and the significance of the effect of mass fraction on diffusion in their systems.[28, 58, 59] However, diffusion of small molecules have been shown to have linear relationship to water content in PEG hydrogels.[58] As all positions within our gradient have a similar water content by 10 days of culture, they should have similar diffusion characteristics by that time point limiting the effect of mass transport on data from that time point on.

OA chondrocytes have been shown to be more prone to apoptosis than healthy chondrocytes.[41, 60] The activation of the extrinsic apoptotic pathway was reduced over time through encapsulating the OA chondrocytes within PEG hydrogels indicating that the hydrogels were able to provide an environment which promoted maintenance of cell number and lead to increased expression of chondrogenic phenotype markers.[41] However, the previous study did not exam the mechanical properties of the hydrogels used, which are known to effect chondrocyte phenotype and behavior[20-23] Changes in the mechanical properties of the matrix have been shown to modulate apoptosis in other cell types [61-63], therefore this mechanically influenced modulation of apoptosis may contribute to the differences in DNA content, chondrogenic phenotype markers and ECM formation observed along the gradient in this study. Changes in substrate mechanical properties have been linked to changes in differentiation in numerous cell types.[64-66] Chondrocyte phenotype was monitored using the ratio of CD14/CD90, which is a more pronounced and quicker to decrease temporally (10,000 fold after 1 passage at the protein level and 1,000 fold after 10 days at the mRNA level) than traditions phenotype indicators, such as collagen type II to I (10 fold after 10 days at the mRNA level) and of aggrecan to versican (5 fold after 10 days at the mRNA level).[46, 47] The CD14/CD90 indicator has also been confirmed at the protein expression level,[43, 47] making it an ideal marker to provide quantitative information on chondrocyte phenotype while maintaining spatial information about cellular location within the gradient. A reduction in the CD14/CD90 ratio due mainly to decreased CD14 expressionwas observed over the entire modulus gradient after 10 days of culture (Figure 3B). However, this reduction was not significant in chondrocytes encapsulated at the 1700 Pa Young's Modulus gradient position, , indicating that this region is better able to maintain phenotype compared to the other regions of the gradient. Additionally, this reduction was delayed compared to previously reported 2D culture across all gradient positions[47] indicating that 3D culture regardless of mechanical properties in the regime tested enhance chondrocyte phenotype maintenance compared to 2D culture.

Chondrocyte phenotype can be effected by changes in cytoskeletal organization and shape.[67] There are zonal differences in actin amount and arrangement in both healthy and OA cartilage[68, 69] which may occur in response to zonal differences in mechanical properties.[12, 13] Specifically, as the mechanical properties of cartilage increase from the superficial to the deep zone, the actin expression within the chondrocytes reduces.[69] Similar to cartilage, chondrocytes in gradient regions with the highest modulus had reduced actin expression compared to chondrocytes in all but the lowest modulus regions within our gradient (Figure 4). Reduced actin intensity in the regions of the lowest modulus could be due to a number of factors such as increased transmittance of shear force to the cells or increased expression of growth factors or ECM proteins due to the effect of reduced mechanical properties on the cells compared to the other gradient regions.[70-73] However, the elucidation of the exact cause is beyond the scope of this study.

Although generally round in shape throughout our gel, which is typical for chondrocytes in 3D culture, differences in actin organization were observed. It is these differences in actin organization, not simply the round shape which modulate chondrocyte phenotype.[51] Actin organization tends to be more localized toward one side cell in regions with reduced stiffness (Figure 4) perhaps reminiscent of the apical organization of actin in healthy

chondrocytes,[74] while in regions with increased storage modulus the cytoskeletal organization of chondrocytes appears less organized cortically (Figure 4) similar to previous reports of OA chondrocytes.[74] As pericellular matrix synthesized and retention of the proteoglycans within cartilage has been linked to actin organization,[75] the variation in actin intensity and organization observed in the Young's modulus gradient (Figure 4) could contribute to the changes in ECM content observed throughout the gradient (Figure 4, 5, 6, 7).

Chondrocytes in 3D culture are often thought to lack focal adhesions. However, the round chondrocyte cytoskeletal structure merely reduces vinculin expression compared to the fibroblastic chondrocyte cytoskeletal structure.[76] Vinculin has been found to be expressed in a punctuated manner co-localized with actin in cartilage and freshly isolated chondrocytes culture on hyaline cartilage.[77, 78] We found a similar punctuated expression primarily in gradient regions with lower Young's modulus (Figure 4), while gradient regions of the higher Young's modulus primarily exhibited a more densely clustered vinculin expression (Figure 4). As reduced vinculin has been observed with increased ECM expression in chondrocytes,[76] the variations in vinculin expression in regions of varying moduli within the gradient could contribute the variations in ECM content in regions of different moduli in the gradient.

Previous studies examining the effect of varying material stiffness on chondrocytes have showed conflicting results. One study found stiffer materials contained increased GAG content compared to softer regions[20] Other studies, which possessed results similar to ours showed softer hydrogels contain more sGAG and collagen than stiffer hydrogels.[79, 80] MMP-13 has been shown to increase in stiffer materials compared to softer ones, similar to our results; while MMP-3 was shown to be unaffected by material properties after 20 days of culture, which is inconsistent with our study.[80] The inconsistency of results indicates that the factors effecting chondrocyte phenotype, and ECM synthesis and degradation are complex and warrant further study. With varying culture conditions, biomaterials, and cell sources, these factors are difficult to elucidate from existing studies. Additional systematic studies, like the one conducted here, are necessary to understand the causes of these effects variations and develop the optimal scaffold for cartilage formation.

5. Conclusion

This work presents the development and characterization of a gradient hydrogel system for the systematic study of mechanical property changes on OA chondrocyte proliferation, phenotype maintenance, and ECM production. After 10 days of culture, the 6500 Pa Young's Modulus gradient position contained significantly less DNA than most of the other gradient positions. A significant decrease in phenotype markers was also observed at the 6500 Pa Young's Modulus gradient position, while the 1700 Pa Young's Modulus gradient position did not experience a significant drop in phenotype markers. Over three weeks of culture, gradient regions with lower Young's modulus experience an increase in ECM content compared to gradient regions with higher Young's modulus. Variations in actin and vinculin amounts and organization where observed within the modulus gradient which could contribute to the differences in chondrogenic phenotype maintenance and ECM expression. Overall, our data indicates that softer tissue engineering scaffolds will stimulate OA chondrocytes ability to secrete more ECM to repair defects and potentially improve integration in autologus chondrocyte transfer. These data are critical in that improving the activation and proliferative activity of autologously harvested cells while maintaining phenotype is necessary for OA chondrocytes to serve as a viable cell source for tissue engineering.

Acknowledgments

The authors gratefully acknowledge research funding from The University of Akron Research Foundation, the Akron Functional Materials Center and RESBIO "Integrated Technology Resource for Polymeric Biomaterials" (NIH-NIBIB & NCMHD P41EB001046) which enabled this work. The authors would also like the thank Leann Speering for overseeing IRB approval and arranging tissue transfers.

7. References

[1]. Lane NE, Brandt K, Hawker G, Peeva E, Schreyer E, Tsuji W, et al. OARSI-FDA initiative: defining the disease state of osteoarthritis. Osteoarthritis and Cartilage. 2011; 19:478–82. [PubMed: 21396464]

[2]. Squires GR, Okouneff S, Ionescu M, Poole AR. The pathobiology of focal lesion development in aging human articular cartilage and molecular matrix changes characteristic of osteoarthritis. Arthritis & Rheumatism. 2003; 48:1261–70. [PubMed: 12746899]

[3]. Lorenz H, Richter W. Osteoarthritis: Cellular and molecular changes in degenerating cartilage. Progress in Histochemistry and Cytochemistry. 2006; 40:135–63. [PubMed: 16759941]

[4]. Garnero P, Ayral X, Rousseau J-C, Christgau S, Sandell LJ, Dougados M, et al. Uncoupling of type II collagen synthesis and degradation predicts progression of joint damage in patients with knee osteoarthritis. Arthritis & Rheumatism. 2002; 46:2613–24. [PubMed: 12384919]

[5]. Simon CG, Lin-Gibson S. Combinatorial and High-Throughput Screening of Biomaterials. Advanced Materials. 2011; 23:369–87. [PubMed: 20839249]

[6]. Peters A, Brey DM, Burdick JA. High-Throughput and Combinatorial Technologies for Tissue Engineering Applications. Tissue Eng Part B-Rev. 2009; 15:225–39. [PubMed: 19290801]

[7]. Cukierman E, Pankov R, Stevens DR, Yamada KM. Taking cell-matrix adhesions to the third dimension. Science. 2001; 294:1708–12. [PubMed: 11721053]

[8]. Tse JR, Engler AJ. Stiffness Gradients Mimicking In Vivo Tissue Variation Regulate Mesenchymal Stem Cell Fate. PLoS One. 2011; 6

[9]. Chatterjee K, Lin-Gibson S, Wallace WE, Parekh SH, Lee YJ, Cicerone MT, et al. The effect of 3D hydrogel scaffold modulus on osteoblast differentiation and mineralization revealed by combinatorial screening. Biomaterials. 2010; 31:5051–62. [PubMed: 20378163]

[10]. Burdick JA, Khademhosseini A, Langer R. Fabrication of Gradient Hydrogels Using a Microfluidics/Photopolymerization Process. Langmuir. 2004; 20:5153–6. [PubMed: 15986641]

[11]. Williamson AK, Chen AC, Sah RL. Compressive properties and function—composition relationships of developing bovine articular cartilage. Journal of Orthopaedic Research. 2001; 19:1113–21. [PubMed: 11781013]

[12]. Darling EM, Zauscher S, Guilak F. Viscoelastic properties of zonal articular chondrocytes measured by atomic force microscopy. Osteoarthritis and Cartilage. 2006; 14:571–9. [PubMed: 16478668]

[13]. Buckley MR, Gleghorn JP, Bonassar LJ, Cohen I. Mapping the depth dependence of shear properties in articular cartilage. Journal of Biomechanics. 2008; 41:2430–7. [PubMed: 18619596]

[14]. Athanasiou KA, Rosenwasser MP, Buckwalter JA, Malinin TI, Mow VC. Interspecies comparisons of in situ intrinsic mechanical properties of distal femoral cartilage. Journal of Orthopaedic Research. 1991; 9:330–40. [PubMed: 2010837]

[15]. Guilak F, Jones WR, Ting-Beall HP, Lee GM. The deformation behavior and mechanical properties of chondrocytes in articular cartilage. Osteoarthritis and Cartilage. 1999; 7:59–70. [PubMed: 10367015]

[16]. Alexopoulos LG, Williams GM, Upton ML, Setton LA, Guilak F. Osteoarthritic changes in the biphasic mechanical properties of the chondrocyte pericellular matrix in articular cartilage. Journal of Biomechanics. 2005; 38:509–17. [PubMed: 15652549]

[17]. Nam J, Johnson J, Lannutti JJ, Agarwal S. Modulation of embryonic mesenchymal progenitor cell differentiation via control over pure mechanical modulus in electrospun nanofibers. Acta Biomater. 2011; 7:1516–24. [PubMed: 21109030]

[18]. Bahney CS, Hsu C-W, Yoo JU, West JL, Johnstone B. A bioresponsive hydrogel tuned to chondrogenesis of human mesenchymal stem cells. The FASEB Journal. 2011; 25:1486–96.

[19]. Roberts JJ, Earnshaw A, Ferguson VL, Bryant SJ. Comparative study of the viscoelastic mechanical behavior of agarose and poly(ethylene glycol) hydrogels. Journal of Biomedical Materials Research Part B: Applied Biomaterials. 2011; 99B:158–69.

[20]. Bryant SJ, Anseth KS. Hydrogel properties influence ECM production by chondrocytes photoencapsulated in poly(ethylene glycol) hydrogels. Journal of Biomedical Materials Research. 2002; 59:63–72. [PubMed: 11745538]

[21]. Miot S, Woodfield T, Daniels AU, Suetterlin R, Peterschmitt I, Heberer M, et al. Effects of scaffold composition and architecture on human nasal chondrocyte redifferentiation and cartilaginous matrix deposition. Biomaterials. 2005; 26:2479–89. [PubMed: 15585250]

[22]. Klein TJ, Rizzi SC, Schrobback K, Reichert JC, Jeon JE, Crawford RW, et al. Long-term effects of hydrogel properties on human chondrocyte behavior. Soft Matter. 2010; 6:5175–83.

[23]. Bryant SJ, Anseth KS, Lee DA, Bader DL. Crosslinking density influences the morphology of chondrocytes photoencapsulated in PEG hydrogels during the application of compressive strain. Journal of Orthopaedic Research. 2004; 22:1143–9. [PubMed: 15304291]

[24]. Ruoslahti E, Pierschbacher MD. ARG-GLY-ASP - A VERSATILE CELL RECOGNITION SIGNAL. Cell. 1986; 44:517–8. [PubMed: 2418980]

[25]. Humphries JD, Byron A, Humphries MJ. Integrin ligands at a glance. J Cell Sci. 2006; 119:3901–3. [PubMed: 16988024]

[26]. Canal T, Peppas NA. Correlation between mesh size and equilibrium degree of swelling of polymeric networks. J Biomed Mater Res. 1989; 23:1183–93. [PubMed: 2808463]

[27]. Lu S, Anseth KS. Release Behavior of High Molecular Weight Solutes from Poly(ethylene glycol)-Based Degradable Networks. Macromolecules. 2000; 33:2509–15.

[28]. Cruise GM, Scharp DS, Hubbell JA. Characterization of permeability and network structure of interfacially photopolymerized poly(ethylene glycol) diacrylate hydrogels. Biomaterials. 1998; 19:1287–94. [PubMed: 9720892]

[29]. Merrill EW, Dennison KA, Sung C. Partitioning and diffusion of solutes in hydrogels of poly(ethylene Oxide). Biomaterials. 1993; 14:1117–26. [PubMed: 8130315]

[30]. Lin DC, Shreiber DI, Dimitriadis EK, Horkay F. Spherical indentation of soft matter beyond the Hertzian regime: numerical and experimental validation of hyperelastic models. Biomechanics and Modeling in Mechanobiology. 2009; 8:345–58. [PubMed: 18979205]

[31]. Chan EP, Hu YH, Johnson PM, Suo ZG, Stafford CM. Spherical indentation testing of poroelastic relaxations in thin hydrogel layers. Soft Matter. 2012; 8:1492–8.

[32]. Morgan AW, Roskov KE, Lin-Gibson S, Kaplan DL, Becker ML, Simon CG. Characterization and optimization of RGD-containing silk blends to support osteoblastic differentiation. Biomaterials. 2008; 29:2556–63. [PubMed: 18325585]

[33]. Strehin, IA.; Elisseeff, JH. Characterizing ECM Production by Cells Encapsulated in Hydrogels. In: Even-Ram, S.; Artym, V., editors. Extracellular Matrix Protocols: Humana Press. 2009. p. 349-62.

[34]. Smith LA, Liu X, Hu J, Ma PX. The influence of three-dimensional nanofibrous scaffolds on the osteogenic differentiation of embryonic stem cells. Biomaterials. 2009; 30:2516–22. [PubMed: 19176243]

[35]. Nugent AE, Reiter DA, Fishbein KW, McBurney DL, Murray T, Bartusik D, et al. Characterization of Ex Vivo–Generated Bovine and Human Cartilage by Immunohistochemical, Biochemical, and Magnetic Resonance Imaging Analyses. Tissue Engineering Part A. 2010; 16:2183–96. [PubMed: 20136403]

[36]. Frazier SB, Roodhouse KA, Hourcade DE, Zhang L. The Quantification of Gycosaminoglycans: A Comparison of HPLC, Carbazole, and Alican Blue Methods. Open Glycosci. 2008; 1:31–9. [PubMed: 20640171]

[37]. Callahan LAS, Ganios AM, McBurney DL, Dilisio MF, Weiner SD, Horton WE, et al. ECM Production of Primary Human and Bovine Chondrocytes in Hybrid PEG Hydrogels Containing Type I Collagen and Hyaluronic Acid. Biomacromolecules. 2012; 13:1625–31. [PubMed: 22559049]

[38]. Karlsson M, Björnsson S. Quantitation of Proteoglycans in Biological Fluids Using Alcian Blue Methods in Molecular Biology. 2001; 171:159–73.

[39]. Bjornsson S. SIMULTANEOUS PREPARATION AND QUANTITATION OF PROTEOGLYCANS BY PRECIPITATION WITH ALCIAN BLUE. Anal Biochem. 1993; 210:282–91. [PubMed: 8512063]

[40]. Nguyen LH, Kudva AK, Saxena NS, Roy K. Engineering articular cartilage with spatially-varying matrix composition and mechanical properties from a single stem cell population using a multi-layered hydrogel. Biomaterials. 2011; 32:6946–52. [PubMed: 21723599]

[41]. Musumeci G, Loreto C, Carnazza M, Strehin I, Elisseeff J. OA cartilage derived chondrocytes encapsulated in poly(ethylene glycol) diacrylate (PEGDA) for the evaluation of cartilage restoration and apoptosis in an in vitro model. Histol Histopathol. 2011; 26:1265–78. [PubMed: 21870330]

[42]. Armstrong C, Mow V. Variations in the intrinsic mechanical properties of human articular cartilage with age, degeneration, and water content. J Bone Joint Surg Am. 1982; 64:88–94. [PubMed: 7054208]

[43]. Diaz-Romero J, Gaillard JP, Grogan SP, Nesic D, Trub T, Mainil-Varlet P. Immunophenotypic analysis of human articular chondrocytes: Changes in surface markers associated with cell expansion in monolayer culture. Journal of Cellular Physiology. 2005; 202:731–42. [PubMed: 15389573]

[44]. Summers KL, Odonnell JL, Hoy MS, Peart M, Dekker J, Rothwell A, et al. MONOCYTE-MACROPHAGE ANTIGEN EXPRESSION ON CHONDROCYTES. J Rheumatol. 1995; 22:1326–34. [PubMed: 7562767]

[45]. Chen XD, Qian HY, Neff L, Satomura K, Horowitz MC. Thy-1 antigen expression by cells in the osteoblast lineage. J Bone Miner Res. 1999; 14:362–75. [PubMed: 10027901]

[46]. Diaz-Romero J, Nesic D, Grogan SP, Heini P, Mainil-Varlet P. Immunophenotypic changes of human articular chondrocytes during monolayer culture reflect bona fide dedifferentiation rather than amplification of progenitor cells. Journal of Cellular Physiology. 2008; 214:75–83. [PubMed: 17559082]

[47]. Giovannini S, Diaz-Romero J, Aigner T, Mainil-Varlet P, Nesic D. Population doublings and percentage of S100-positive cells as predictors of in vitro chondrogenicity of expanded human articular chondrocytes. Journal of Cellular Physiology. 2010; 222:411–20. [PubMed: 19890919]

[48]. Benya PD, Padilla SR. Dihydrocytochalasin B Enhances Transforming Growth Factor-[beta]-Induced Reexpression of the Differentiated Chondrocyte Phenotype without Stimulation of Collagen Synthesis. Experimental Cell Research. 1993; 204:268–77. [PubMed: 8440324]

[49]. Benya PD, Brown PD, Padilla SR. Microfilament modification by dihydrocytochalasin B causes retinoic acid-modulated chondrocytes to reexpress the differentiated collagen phenotype without a change in shape. The Journal of Cell Biology. 1988; 106:161–70. [PubMed: 3276711]

[50]. Loty S, Forest N, Boulekbache H, Sautier J-M. Cytochalasin D induces changes in cell shape and promotes in vitro chondrogenesis: A morphological study. Biology of the Cell. 1995; 83:149–61. [PubMed: 7549910]

[51]. Brown PD, Benya PD. Alterations in chondrocyte cytoskeletal architecture during phenotypic modulation by retinoic acid and dihydrocytochalasin B-induced reexpression. The Journal of Cell Biology. 1988; 106:171–9. [PubMed: 3276712]

[52]. Place ES, Evans ND, Stevens MM. Complexity in biomaterials for tissue engineering. Nat Mater. 2009; 8:457–70. [PubMed: 19458646]

[53]. Smith LA, Liu XH, Ma PX. Tissue engineering with nano-fibrous scaffolds. Soft Matter. 2008; 4:2144–9. [PubMed: 20052297]

[54]. Mitragotri S, Lahann J. Physical approaches to biomaterial design. Nat Mater. 2009; 8:15–23. [PubMed: 19096389]

[55]. Engler AJ, Sen S, Sweeney HL, Discher DE. Matrix Elasticity Directs Stem Cell Lineage Specification. Cell. 2006; 126:677–89. [PubMed: 16923388]

[56]. Brown TD, Singerman RJ. Experimental determination of the linear biphasic constitutive coefficients of human fetal proximal femoral chondroepiphysis. Journal of Biomechanics. 1986; 19:597–605. [PubMed: 3771582]

[57]. Mow VC, Holmes MH, Michael Lai W. Fluid transport and mechanical properties of articular cartilage: A review. Journal of Biomechanics. 1984; 17:377–94. [PubMed: 6376512]

[58]. Kristin E, Curtis WF. Protein diffusion in photopolymerized poly(ethylene glycol) hydrogel networks. Biomedical Materials. 2011; 6:055006. [PubMed: 21873762]

[59]. Brandl F, Kastner F, Gschwind RM, Blunk T, Teßmar J, Göpferich A. Hydrogel-based drug delivery systems: Comparison of drug diffusivity and release kinetics. Journal of Controlled Release. 2010; 142:221–8. [PubMed: 19887092]

[60]. Musumeci G, Loreto C, Carnazza ML, Martinez G. Characterization of apoptosis in articular cartilage derived from the knee joints of patients with osteoarthritis. Knee Surg Sports Traumatol Arthrosc. 2011; 19:307–13. [PubMed: 20644910]

[61]. Leight JL, Wozniak MA, Chen S, Lynch ML, Chen CS. Matrix rigidity regulates a switch between TGF-β1–induced apoptosis and epithelial–mesenchymal transition. Molecular Biology of the Cell. 2012; 23:781–91. [PubMed: 22238361]

[62]. Wang H-B, Dembo M, Wang Y-L. Substrate flexibility regulates growth and apoptosis of normal but not transformed cells. American Journal of Physiology - Cell Physiology. 2000; 279:C1345–C50. [PubMed: 11029281]

[63]. Tilghman RW, Cowan CR, Mih JD, Koryakina Y, Gioeli D, Slack-Davis JK, et al. Matrix Rigidity Regulates Cancer Cell Growth and Cellular Phenotype. PLoS ONE. 2010; 5:e12905. [PubMed: 20886123]

[64]. Peyton SR, Raub CB, Keschrumrus VP, Putnam AJ. The use of poly(ethylene glycol) hydrogels to investigate the impact of ECM chemistry and mechanics on smooth muscle cells. Biomaterials. 2006; 27:4881–93. [PubMed: 16762407]

[65]. Khatiwala CB, Peyton SR, Metzke M, Putnam AJ. The regulation of osteogenesis by ECM rigidity in MC3T3-E1 cells requires MAPK activation. Journal of Cellular Physiology. 2007; 211:661–72. [PubMed: 17348033]

[66]. Parekh SH, Chatterjee K, Lin-Gibson S, Moore NM, Cicerone MT, Young MF, et al. Modulus-driven differentiation of marrow stromal cells in 3D scaffolds that is independent of myosin-based cytoskeletal tension. Biomaterials. 2011; 32:2256–64. [PubMed: 21176956]

[67]. Daniels K, Solursh M. Modulation of chondrogenesis by the cytoskeleton and extracellular matrix. J Cell Sci. 1991; 100:249–54. [PubMed: 1757484]

[68]. Kouri JB, Arg, uuml, ello C, Luna J, et al. Use of microscopical techniques in the study of human chondrocytes from osteoarthritic cartilage: An overview. Microscopy Research and Technique. 1998; 40:22–36. eacute. [PubMed: 9443154]

[69]. Langelier E, Suetterlin R, Hoemann CD, Aebi U, Buschmann MD. The Chondrocyte Cytoskeleton in Mature Articular Cartilage: Structure and Distribution of Actin, Tubulin, and Vimentin Filaments. Journal of Histochemistry & Cytochemistry. 2000; 48:1307–20. [PubMed: 10990485]

[70]. Ofek G, Dowling EP, Raphael RM, McGarry JP, Athanasiou KA. Biomechanics of single chondrocytes under direct shear. Biomechanics and Modeling in Mechanobiology. 2010; 9:153–62. [PubMed: 19644718]

[71]. Leipzig ND, Eleswarapu SV, Athanasiou KA. The effects of TGF-β1 and IGF-I on the biomechanics and cytoskeleton of single chondrocytes. Osteoarthritis and Cartilage. 2006; 14:1227–36. [PubMed: 16824771]

[72]. Qusous A, Parker E, Geewan C, Kapasi A, Getting SJ, Hucklebridge F, et al. Novel methods for the quantification of changes in actin organization in chondrocytes using fluorescent imaging and linear profiling. Microscopy Research and Technique. 2012 n/a-n/a.

[73]. Campbell JJ, Blain EJ, Chowdhury TT, Knight MM. Loading alters actin dynamics and up-regulates cofilin gene expression in chondrocytes. Biochemical and Biophysical Research Communications. 2007; 361:329–34. [PubMed: 17662250]

[74]. Fioravanti A, Nerucci F, Annefeld M, Collodel G, Marcolongo R. Morphological and cytoskeletal aspects of cultivated normal and osteoarthritic human articular chondrocytes after cyclical pressure: a pilot study. Clin Exp Rheumatol. 2003; 21:739–46. [PubMed: 14740453]

[75]. Nofal GA, Knudson CB. Latrunculin and Cytochalasin Decrease Chondrocyte Matrix Retention. Journal of Histochemistry & Cytochemistry. 2002; 50:1313–23. [PubMed: 12364564]

[76]. Mahmood TA, de Jong R, Riesle J, Langer R, van Blitterswijk CA. Adhesion-mediated signal transduction in human articular chondrocytes: the influence of biomaterial chemistry and tenascin-C. Experimental Cell Research. 2004; 301:179–88. [PubMed: 15530854]

[77]. Durrant LA, Archer CW, Benjamin M, Ralphs JR. Organisation of the chondrocyte cytoskeleton and its response to changing mechanical conditions in organ culture. Journal of Anatomy. 1999; 194:343–53. [PubMed: 10386772]

[78]. Wang H, Kandel RA. Chondrocytes attach to hyaline or calcified cartilage and bone. Osteoarthritis and Cartilage. 2004; 12:56–64. [PubMed: 14697683]

[79]. Schuh E, Hofmann S, Stok K, Notbohm H, Müller R, Rotter N. Chondrocyte redifferentiation in 3D: The effect of adhesion site density and substrate elasticity. Journal of Biomedical Materials Research Part A. 2012; 100A:38–47. [PubMed: 21972220]

[80]. Nicodemus GD, Skaalure SC, Bryant SJ. Gel structure has an impact on pericellular and extracellular matrix deposition, which subsequently alters metabolic activities in chondrocyte-laden PEG hydrogels. Acta Biomater. 2011; 7:492–504. [PubMed: 20804868]

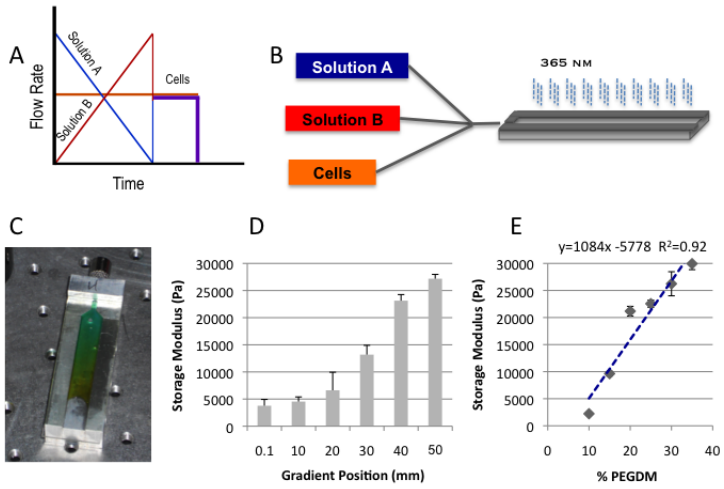

Figure 1.

Depicts the overall framework and assembly of the gradient fabrication system. Schematic of the controlled variation in syringe pump rates coupled with a constant rate of cell infusion which ensures uniform cell density throughout the gradient **A)**; a schematic for the three component (expandable to five) gradient fabrication system **B)**; and an example of the gradient profile that can be generated depicted with a colorimetric gradient for visualization purposes **C)**. The storage modulus can be controlled systematically enabling facile correlations of mechanical properties via position **D)**. The positional values correlate well with values obtained from discrete hydrogel standards of known composition and mass fraction **E)**. Mass fraction, pore size, transitional dimensions are controlled by defined solution mixtures pre-loaded in syringe pumps.

A

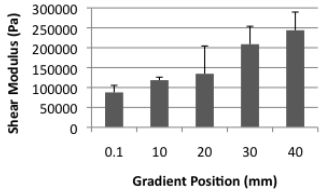

B

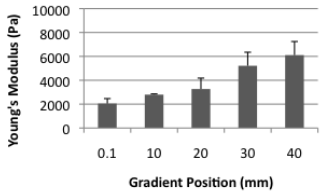

C

Gradient Position	Swelling Volume	Mesh Size (A)
0	13.4 ± 1.7	116.7 ± 11.4
5	12.7 ± 1.0	112.5 ± 5.4
10	12.3 ± 0.8	109.2 ± 3.7
15	10.8 ± 0.6	92.0 ± 8.0
20	10.6 ± 0.7	89.3 ± 0.6
25	9.7 ± 0.5	79.5 ± 1.2
30	9.1 ± 0.9	71.9 ± 13.0
35	8.6 ± 0.8	54.7 ± 4.0
40	8.5 ± 0.8	53.2 ± 5.0
45	7.8 ± 0.2	52.4 ± 6.5

Figure 2.

Characterization of all hydrogel physical properties can be correlated to position within the gradient via the highly reproducible fabrication process **A)** Shear Modulus **B)** Young's Modulus and **C)** Table of swelling volume and calculated mesh size after 24 h of swelling.

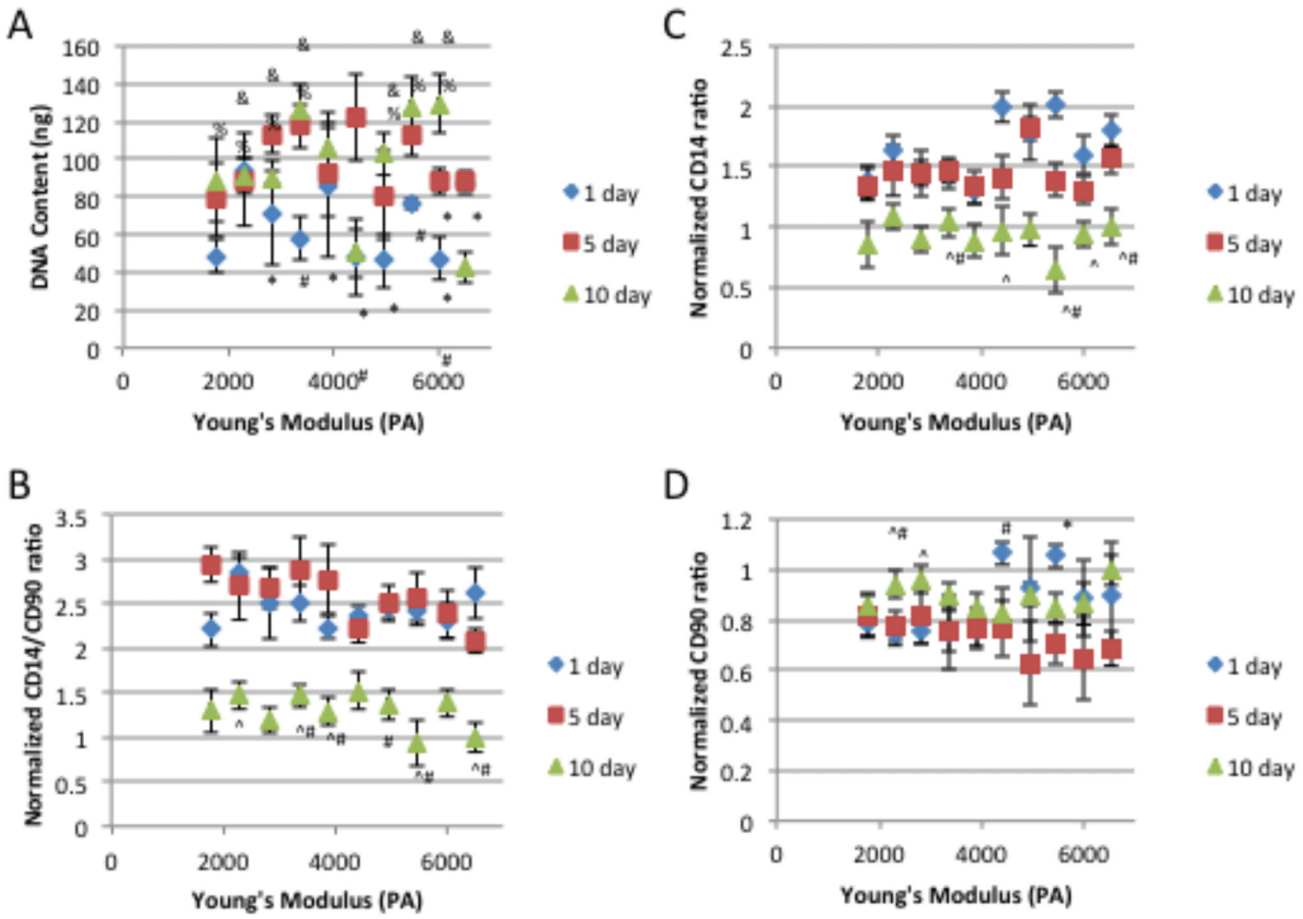

Figure 3.

Chondrocyte **A**) DNA content , phenotype maintenance indicator **B)** CD14/CD90 ratio, **C)** cellular fraction expressing CD14 and **D)** cellular fraction expressing CD90 over 10 days of culture. * indicates a p-value ≤ 0.05 compared to the value at day 10 within the same gradient position, # indicates a p-value ≤ 0.05 compared to the value at day 5 within the same gradient position, ^ indicates a p-value ≤ 0.05 compared to the value at day 1 within the same gradient position, % indicates a p-value ≤ 0.05 compared to 6500 Pa Young's Modulus gradient position at day 10, and & indicates a p-value ≤ 0.05 compared to 4400 Pa Young's Modulus gradient position at day 10.

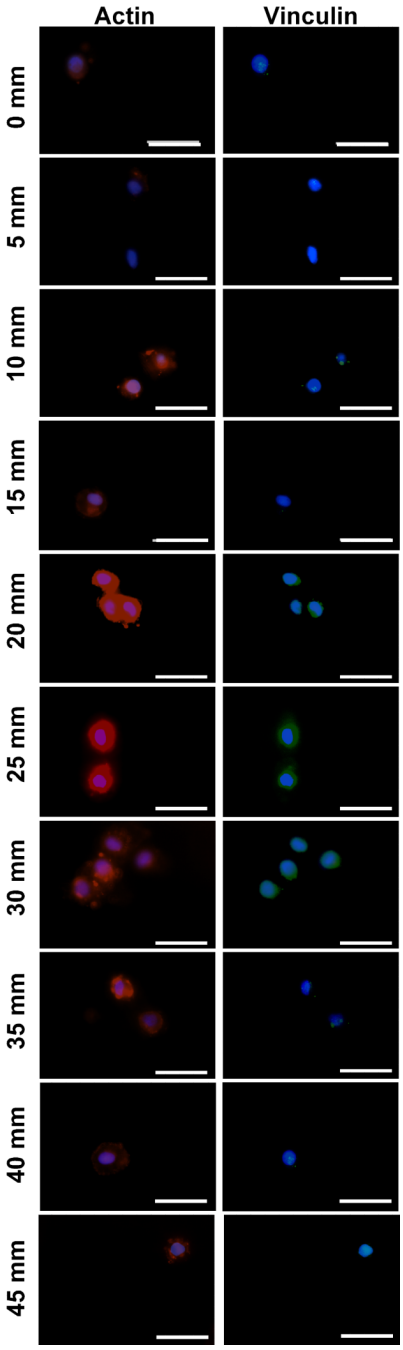

Figure 4.
Specific staining for the cytoskeletal elements actin (Red), vinculin (Green) and nuclear (blue) after 5 days of culture show distinct morphometric changes as the modulus changes from a low modulus (0 mm) to a high modulus (45 mm) position. Scale bar = 25 μM

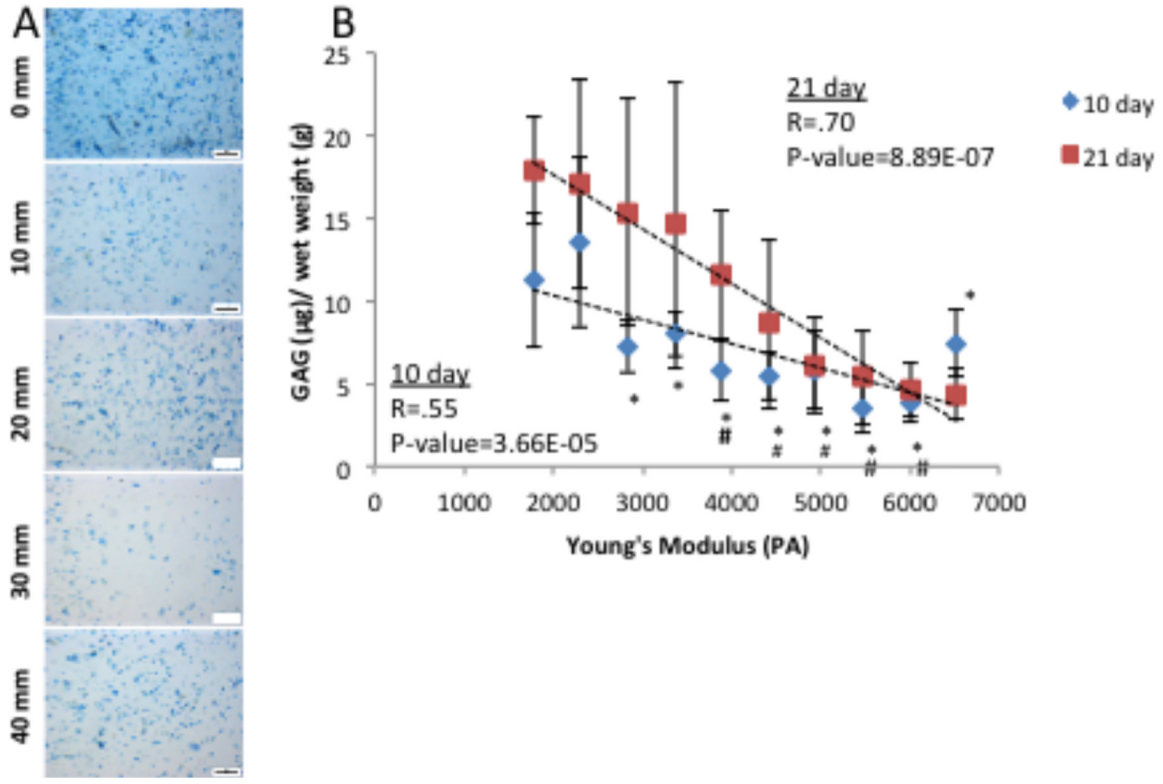

Figure 5.

Extracellular matrix production by human chondrocytes after 10 days of culture. Images were taken at 10 mm intervals along the length of the modulus gradient. **A)** Whole mount Alcian blue and **B)** Sulfated gylcosaminoglycan quantification based on Alcian blue extraction show distinct changes with position in the modulus profile at both 10 day and 21 days. Scale bar = 200 μm. # indicates a p-value ≤ 0.05 compared to 1700 Pa Young's Modulus gradient position, and * indicates a p-value ≤ 0.05 compared to 2300 Pa Young's Modulus gradient position

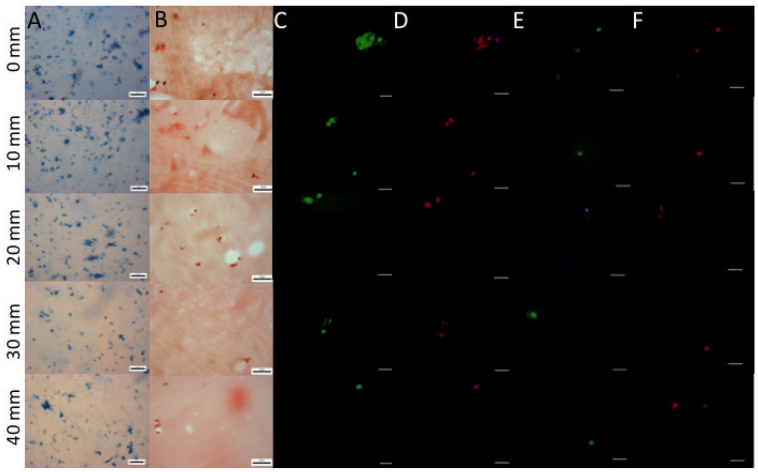

Figure 6.

Extracellular matrix production by human chondrocytes after 3 weeks of culture. Images where taken every 5mm down the length of the gradient **A)** Whole mount Alcian Blue staining. Scale bar = 200 μm. **B)** Sirius red staining of histological sections. Scale bar = 50 μm. **C)** Type 2 Collagen (green) and nuclear (blue) immunofluorescence of histological sections. Scale bar = 25 μm. **D)** Type 1 Collagen (red) and nuclear (blue) immunofluorescence of histological sections. Scale bar = 25 μm. **E)** matrix metalloprotease 13 (green) and nuclear (blue) immunofluorescence of histological sections. Scale bar = 25 μm. **F)** matrix metalloprotease 3 (red) and nuclear (blue) immunofluorescence of histological sections. Scale bar = 25 μm.

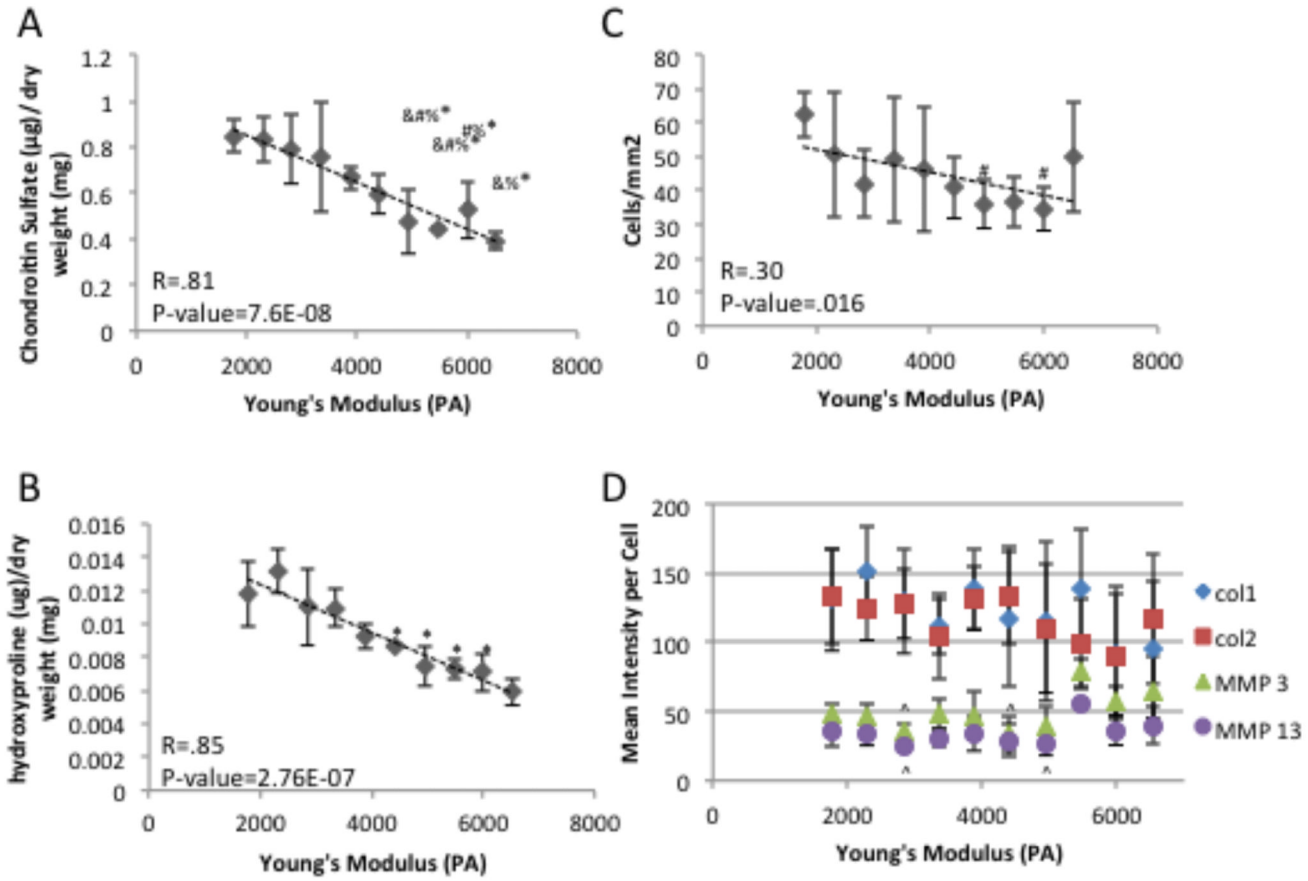

Figure 7.

Quantification of extracellular matrix after 3 weeks of culture **A)** Sulfated gylcosaminoglycan dimethylmethlene blue biochemical quantification. B) Hydroxyproline biochemical quantification. **C)** quantification of cellular number present in histological samples **D)** mean gray scale intensity for immunoflorescence staining of collagen type 1 & 2, matrix metalloprotease 3 & 13 for chondrocytes in histological samples. # indicates a p-value ≤ 0.05 compared to 1700 Pa Young's Modulus gradient position, * indicates a p-value ≤ 0.05 compared to 2300 Pa Young's Modulus gradient position, % indicates a p-value ≤ 0.05 compared to 2800 Pa Young's Modulus gradient position, & indicates a p-value ≤ 0.05 compared to 3400 Pa Young's Modulus gradient position, and ^ indicate a a p-value ≤ 0.05 compared to 5500 Pa Young's Modulus gradient position.